Charge-Density-Wave Destruction and Ferromagnetic Order in $SmNiC_2$

S. Shimomura,[1] C. Hayashi,[1] G. Asaka,[1] N. Wakabayashi,[1] M. Mizumaki,[2] and H. Onodera[3]

[1]*Department of Physics, Faculty of Science and Technology, Keio University, 3-14-1 Hiyoshi, Kohoku-ku, Yokohama 223-8522, Japan*
[2]*SPring-8/JASRI, 1-1-1 Kouto, Sayo, Hyogo 679-5198, Japan*
[3]*Department of Physics, Graduate School of Science, Tohoku University, Sendai 980-8578, Japan*

(Received 6 August 2008; published 19 February 2009)

X-ray scattering and electrical resistivity measurements were performed on $SmNiC_2$. Satellite peaks characterized by an incommensurate wave vector (0.5, η, 0) appear below 148 K, at which the resistivity shows an anomaly. The temperature dependence of thermal diffuse scattering above 148 K suggests critical phonon softening. These results indicate the formation of a charge-density-wave. The satellite peaks abruptly disappear and the resistivity sharply decreases when a ferromagnetic transition takes place at 17.7 K.

DOI: 10.1103/PhysRevLett.102.076404 PACS numbers: 71.45.Lr, 61.44.Fw, 64.70.Rh, 75.50.Cc

The charge-density-wave (CDW) transition originates from electron-lattice interaction in low-dimensional metallic systems [1]. The nesting of the Fermi surface leads to electronic instability resulting in a charge density modulation accompanied by a periodic lattice distortion characterized by the wave vector $2\boldsymbol{k}_F$, where $\boldsymbol{k}_F$ is the Fermi wave vector. A Kohn anomaly is formed in a phonon branch, and critical phonon softening occurs. Many investigations have been performed to understand the competition between the CDW and superconductivity in various compounds. The interrelationship between the CDW and magnetism is also an interesting subject, because fascinating phenomena, such as large magnetoresistance, can be expected to occur. This interrelationship may be realized in low-dimensional rare-earth metal compounds through the electron-lattice interaction and the magnetic interaction between local moments of $4f$ electrons mediated by conduction electrons. Some rare-earth compounds exhibiting CDW transitions have been reported, and there is no evident coupling between the CDW and the magnetic ordering [2–4].

Murase *et al.* [5] found that rare-earth intermetallic compounds $R\mathrm{NiC}_2$ (R denotes a rare-earth-metal element), which have an orthorhombic CeNiC_2-type structure (space group $Amm2$) [6–8], show anomalous temperature dependences of electrical resistivity and lattice constants. They suggested that these anomalies are attributed to CDW transitions. However, no experimental evidence of the CDW states has been obtained from x-ray and neutron diffraction experiments. The R local moments order antiferromagnetically in most of the $R\mathrm{NiC}_2$ compounds, and $SmNiC_2$ undergoes a first-order ferromagnetic transition at $T_C = 17.5$ K [9–17].

Here, we report experimental evidence of the CDW formation and its destruction in $SmNiC_2$. The observation of an incommensurate lattice modulation and its critical fluctuation using x-ray diffraction and diffuse scattering suggests that a CDW state is formed below 148 K. Surprisingly, the CDW lattice modulation disappears below T_C, accompanied by a sharp decrease in the electrical resistivity by a factor of 10. We propose that $SmNiC_2$ is a unique example of a system characterized by the interplay between the CDW and the magnetic ordering.

The compound $SmNiC_2$ was synthesized by the procedure reported previously [10–12]. The obtained ingots consisted of a large number of single-crystal grains. Measurements of DC electrical resistivities along the a, b, and c axes were performed by the standard four-probe method using a closed-cycle refrigerator. Each sample was cut so that most of the sample volume was a favorable domain. The typical sample size was $0.8 \times 0.7 \times 4.2$ mm^3. X-ray diffraction and diffuse scattering measurements were carried out using synchrotron radiation at BL46XU of SPring-8. The x-ray energy was 18 keV. A sample was prepared in the form of a plate with the surface parallel to the (010) plane. The sample size was $1.8 \times 1.7 \times 0.5$ mm^3. The sample was attached on a cold finger of a closed-cycle refrigerator. A four-axis diffractometer was used, and intensity data were collected by a scintillation detector.

Figure 1 shows the temperature dependences of the electrical resistivities ρ_a, ρ_b, and ρ_c along the a, b, and c axes, respectively. The resistivities are anisotropic ($\rho_c > \rho_b > \rho_a$) with $\rho_c/\rho_a \approx 5.0$ and $\rho_b/\rho_a \approx 2.8$ estimated at 290 K. The anisotropy is relatively low in comparison with those of typical CDW systems, such as $NbSe_3$ [18]. The temperature dependences along the three axes are qualitatively similar to each other: sharp inflections at $T_1 = 148$ K and local maxima at approximately 110 K can be seen. These dependences agree with the result of a previous measurement performed using a polycrystalline sample [5]. The present measurements revealed sharp decreases in the resistivities by a factor of 10 at the ferromagnetic transition temperature. The inset of Fig. 1 shows the resistivities below 30 K. The transition temperatures for cooling and heating, as determined from the resistivity data, are 17.6(1) and 17.8(1) K, respectively. No anomalies

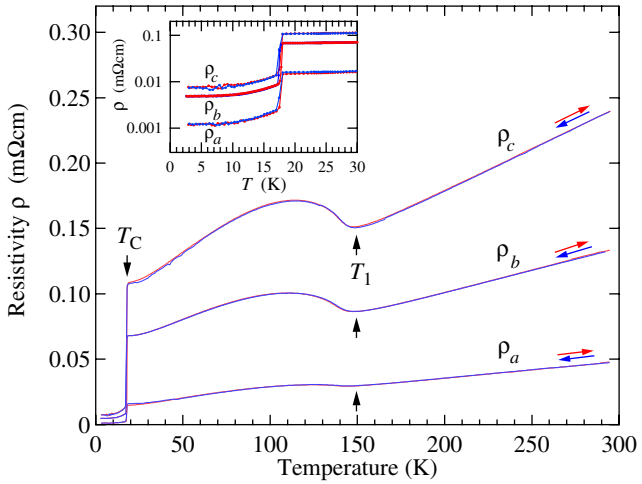

FIG. 1 (color online). Temperature dependences of the electrical resistivities ρ_a, ρ_b, and ρ_c measured along the a, b, and c axes, respectively. The inset shows the resistivities below 30 K.

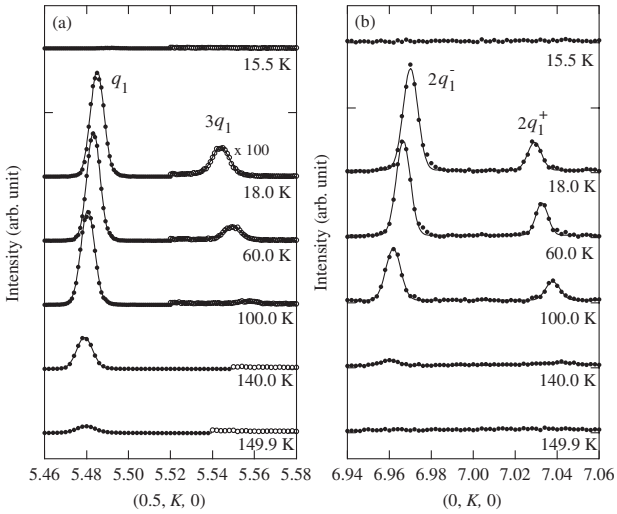

FIG. 2. Temperature dependences of a satellite peak and higher harmonics along the b^*-direction. (a) The satellite peak characterized by $\boldsymbol{q}_1 = (0.5, \eta, 0)$ appears below T_1. A third-order satellite peak, denoted by $3\boldsymbol{q}_1$, can also be seen. (b) Temperature dependence of second-order satellite peaks characterized by $2\boldsymbol{q}_1$, denoted by $2\boldsymbol{q}_1^-$ and $2\boldsymbol{q}_1^+$. All the peaks disappear below T_C.

can be seen at 4.3 K, where small changes in the magnetizations along the three axes were observed [12]. Specific heat measurements using the relaxation method showed no anomaly at 4.3 K [19]. These results indicate that a phase transition does not occur at 4.3 K.

The x-ray diffraction measurements using synchrotron radiation revealed that satellite peaks at $(h, k, l) \pm (0.5, \pm\eta, 0)$ with $\eta \approx 0.52$, characterized by a reduced modulation wave vector $\boldsymbol{q}_1 = (0.5, \eta, 0)$, appear below T_1. We measured the temperature dependence of the satellite peak at $(0.5, 6 - \eta, 0)$. The profiles observed along the b^*-direction at several temperatures are shown in Fig. 2(a). Higher harmonics were also observed. The temperature dependences of the second-order ($2\boldsymbol{q}_1$) and third-order ($3\boldsymbol{q}_1$) satellite peaks are shown in Figs. 2(b) and 2(a), respectively. The $\boldsymbol{q}_1$ satellite peak appears below T_1. As the temperature decreases toward T_C, the $\boldsymbol{q}_1$ satellite peak increases in intensity while shifting its position. The appearance of the satellite peaks suggests that the sharp inflection of the resistivity curve at T_1 is due to the formation of the CDW state leading to the opening of a partial gap at the Fermi level. The satellite peaks characterized by $\boldsymbol{q}_1$, $2\boldsymbol{q}_1$, and $3\boldsymbol{q}_1$ suddenly disappear below T_C. We carried out several scans along specific directions in the reciprocal space below T_C, and no satellite peaks were found [20]. The destruction of the CDW state is consistent with the abrupt decrease in the resistivity at T_C.

Well-defined diffuse scattering centered at $\boldsymbol{q}_1$ was found to exist even at room temperature. Figure 3 shows typical diffuse scattering profiles along the b^*-direction at several temperatures. The intensity increases with decreasing temperature, and the diffuse scattering develops into the $\boldsymbol{q}_1$ satellite peak at T_1. The increase in the diffuse scattering intensity indicates that the phonon frequency ω decreases as the temperature decreases toward T_1, because the thermal diffuse scattering intensity is approximately proportional to $\omega^{-2}(\boldsymbol{q})$ [21].

The temperature dependences of the intensities of the satellite peaks are shown in Fig. 4(a). The integrated intensity of the $\boldsymbol{q}_1$ satellite peak increases monotonically with decreasing temperature and saturates below 80 K. The diffuse scattering intensity at $\boldsymbol{q}_1$, shown in the inset of Fig. 4(a), increases as the temperature decreases toward T_1. The intensities of the $2\boldsymbol{q}_1$ and $3\boldsymbol{q}_1$ satellite peaks substantially increase at lower temperatures, suggesting the squaring-up of the CDW lattice modulation. All the satellite peaks abruptly vanish below T_C. As shown in Fig. 4(b), the value of η changes with temperature, and no apparent lock-in behavior is observed. The temperature dependence of the half width at half maximum (HWHM) of the $\boldsymbol{q}_1$ satellite peak and diffuse scattering is shown in

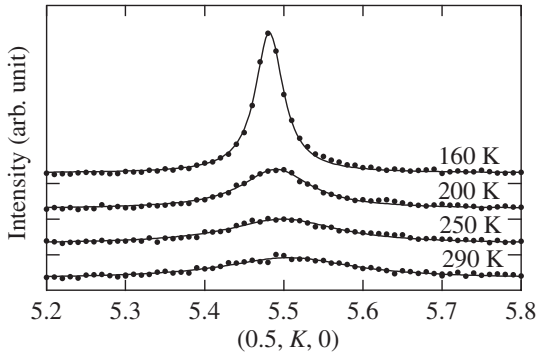

FIG. 3. Temperature dependence of the diffuse scattering profiles characterized by $\boldsymbol{q}_1$ along the b^*-direction.

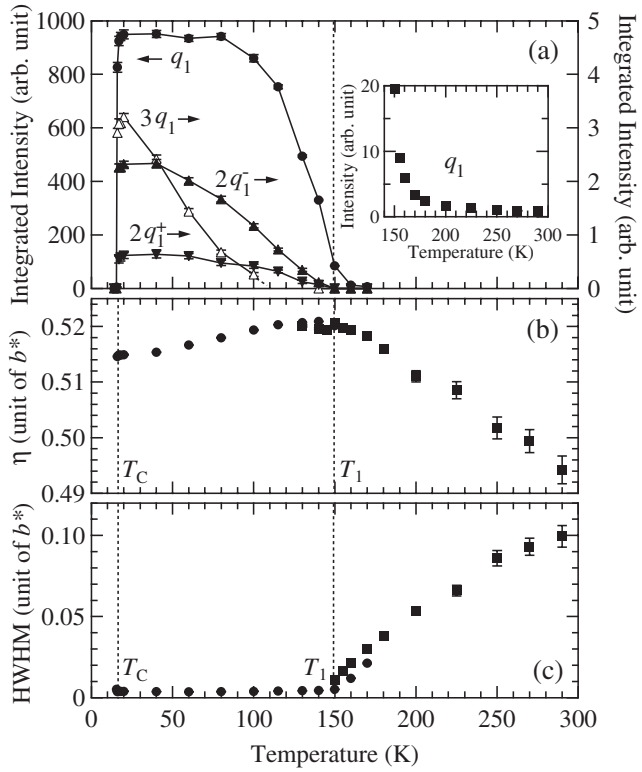

FIG. 4. (a) Temperature dependences of the integrated intensities of $\boldsymbol{q}_1$ and higher-order $2\boldsymbol{q}_1$ ($2\boldsymbol{q}_1^-$ and $2\boldsymbol{q}_1^+$) and $3\boldsymbol{q}_1$ satellite peaks. The inset shows diffuse scattering intensity at $\boldsymbol{q}_1$. Temperature dependences of the value of η and the half width at half maximum (HWHM) of the $\boldsymbol{q}_1$ satellite peak and diffuse scattering are shown in (b) and (c), respectively. The circles and squares represent the results obtained by separate measurements.

Fig. 4(c). The width decreases with decreasing temperature, and it is resolution limited below T_1.

Figure 5 shows a contour plot of the diffuse scattering intensity in the (0.5, K, L) plane measured at 160 K. The diffuse scattering intensity distribution is spread along the c^*-direction. Diffuse scattering centered at (0.5, 5.5, 0.5) and (0.5, 5.5, 1.5), characterized by $\boldsymbol{q}_R = (0.5, 0.5, 0.5)$, exists as well as the more intense $\boldsymbol{q}_1$ diffuse scattering at $L = 0$, 1, and 2. The diffuse scattering profiles along the b^*-direction passing through $(-0.5, 3.5, 0.5)$ and (0.5, 5.5, 0.5) were measured at various temperatures. As shown in Fig. 6(a), the diffuse scattering intensity increases as the temperature decreases toward T_1, suggesting that the phonon frequency at $\boldsymbol{q}_R$ decreases as well as that at $\boldsymbol{q}_1$. In the temperature range between T_1 and T_C, the diffuse scattering intensity does not show monotonic temperature dependence. The diffuse scattering at $\boldsymbol{q}_R$ also vanishes below T_C. As shown in Fig. 6(b), the width decreases monotonically with decreasing temperature. The width does not, however, reach the experimental resolution; the width at 20 K, slightly above T_C, is about 3 times larger than the experimental resolution. A transition to a long-range CDW state characterized by $\boldsymbol{q}_R$ does not take place. This corresponds to the lack of anomalies in the temperature dependences of the resistivities.

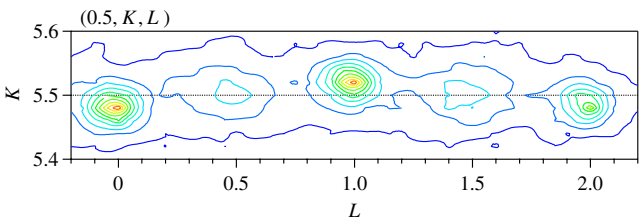

FIG. 5 (color online). Contour plot of x-ray diffuse scattering intensity distribution in the (0.5, K, L) plane measured at 160 K. The scale of the K axis is enlarged in comparison with that of the L axis for the sake of clarity.

The temperature dependence of the magnetic susceptibility of $SmNiC_2$ has been reported [12], and no anomaly was found at T_1. This can be explained by the fact that the change in the Pauli paramagnetism is too small in comparison with the large moment contribution of the Sm ions. Note that there is no anomalous effect of the CDW formation on the magnetic properties at T_1.

As shown in Fig. 1, the resistivity values below T_C appear to be smaller than those extrapolated from the data above T_1. A large modification of the band structure is likely to occur when the first-order ferromagnetic transition takes place. This assumption is consistent with the fact that not only the $\boldsymbol{q}_1$-CDW state but also the $\boldsymbol{q}_R$-CDW fluctuation disappears below T_C. Discontinuous changes in the lattice constants at T_C have been reported [5] and confirmed in the present x-ray experiments. The magnetoelastic coupling, which accounts for first-order magnetic

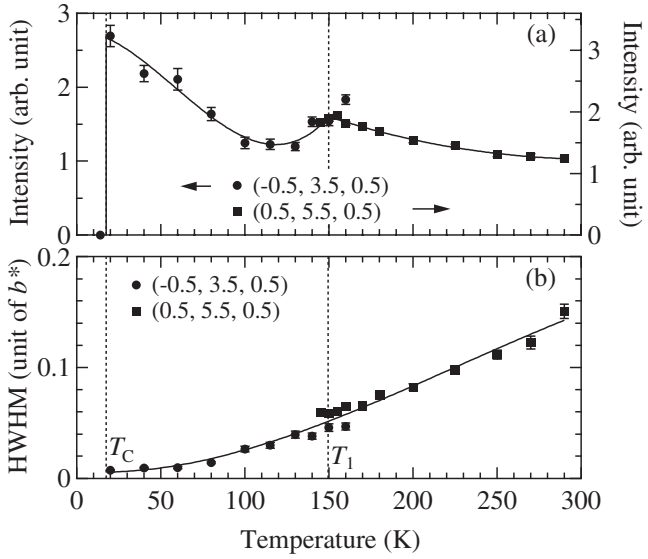

FIG. 6. Temperature dependences of (a) peak intensities and (b) widths of the diffuse scattering centered at $(-0.5, 3.5, 0.5)$ and (0.5, 5.5, 0.5), characterized by $\boldsymbol{q}_R = (0.5, 0.5, 0.5)$. Solid lines are guides for the eye.

transitions accompanied by the lattice distortion, may contribute to the changes in the lattice constants. The lattice change due to the ferromagnetic ordering may modify the electronic structure and affect the nesting condition of the Fermi surface.

Some rare-earth compounds having CDW transitions have been investigated, and no experimental evidence of a relationship between the CDW and magnetic ordering such as that observed in $SmNiC_2$ has been reported. A series of compounds $R_5Ir_4Si_{10}$ [4] has properties similar to those of $SmNiC_2$: the magnetic species are only the R ions, and the CDW transition temperatures are higher than the magnetic transition temperatures. Galli *et al.* showed the coexistence of the CDW and antiferromagnetic order in $Er_5Ir_4Si_{10}$ by observations of CDW reflections and magnetic superlattice reflections [3]. The magnetic transition of this compound, in contrast to $SmNiC_2$, is of second order [3,22]. This implies that the origin of the first-order transition is indeed the key to understanding the destruction of the CDW in $SmNiC_2$. The $RNiC_2$ compounds with $R =$ Nd, Gd, and Tb having antiferromagnetic orders [11–15] show inflections of resistivity curves similar to those observed at T_1 in $SmNiC_2$ [5]. Systematic studies of $RNiC_2$ should provide a comprehensive understanding of the effects of various types of magnetic orders on CDW states.

In summary, x-ray diffraction experiments on $SmNiC_2$ have revealed that satellite peaks characterized by $\boldsymbol{q}_1 = (0.5, \eta, 0)$ appear below $T_1 = 148$ K and that they vanish below $T_C = 17.7$ K. The temperature dependence of the electrical resistivity shows a sharp inflection at T_1 and an abrupt change at T_C. These results can be interpreted as the formation and destruction of a CDW state. The temperature dependence of thermal diffuse scattering suggests critical phonon softening leading to the CDW transition. The compound $SmNiC_2$ is a novel system characterized by the interplay between the CDW and the magnetic ordering. Experimental and theoretical studies that provide information on the Fermi surface are necessary for understanding the formation and destruction of the CDW in $SmNiC_2$.

We are grateful to H. Kuwahara for his helpful advice in the resistivity measurements and to H. Ohsumi and Y. Hirano for their help in the x-ray diffraction experiments. The synchrotron radiation experiments were performed at SPring-8 with the approval of the Japan Synchrotron Radiation Research Institute (JASRI) (Proposal Nos. 2005B0300 and 2006A1255).

[1] G. Grüner, *Density Waves in Solids* (Addison-Wesley, Reading, MA, 1994).

[2] F. Galli, S. Ramakrishnan, T. Taniguchi, G. J. Nieuwenhuys, J. A. Mydosh, S. Geupel, J. Lüdecke, and S. van Smaalen, Phys. Rev. Lett. **85**, 158 (2000).

[3] F. Galli, R. Feyerherm, R. W. A. Hendrikx, E. Dudzik, G. J. Nieuwenhuys, S. Ramakrishnan, S. D. Brown, S. van Smaalen, and J. A. Mydosh, J. Phys. Condens. Matter **14**, 5067 (2002).

[4] S. van Smaalen, M. Shaz, L. Palatinus, P. Daniels, F. Galli, G. J. Nieuwenhuys, and J. A. Mydosh, Phys. Rev. B **69**, 014103 (2004).

[5] M. Murase, A. Tobo, H. Onodera, Y. Hirano, T. Hosaka, S. Shimomura, and N. Wakabayashi, J. Phys. Soc. Jpn. **73**, 2790 (2004).

[6] O. I. Bodak and E. P. Marusin, Dokl. Akad. Nauk Ukr. SSR, Ser. A **12**, 1048 (1979).

[7] K. N. Semenenko, A. A. Putyatin, I. V. Nikol'skaya, and V. V. Burnasheva, Russ. J. Inorg. Chem. **28**, 943 (1983).

[8] W. Jeitschko and M. H. Gerss, J. Less-Common Met. **116**, 147 (1986).

[9] H. Onodera, M. Ohashi, H. Amanai, S. Matsuo, H. Yamauchi, Y. Yamaguchi, S. Funahashi, and Y. Mori, J. Magn. Magn. Mater. **149**, 287 (1995).

[10] Y. Koshikawa, H. Onodera, M. Kosaka, H. Yamauchi, M. Ohashi, and Y. Yamaguchi, J. Magn. Magn. Mater. **173**, 72 (1997).

[11] H. Onodera, N. Uchida, M. Ohashi, H. Yamauchi, Y. Yamaguchi, and N. Sato, J. Magn. Magn. Mater. **137**, 35 (1994).

[12] H. Onodera, Y. Koshikawa, M. Kosaka, M. Ohashi, H. Yamauchi, and Y. Yamaguchi, J. Magn. Magn. Mater. **182**, 161 (1998).

[13] S. Matsuo, H. Onodera, M. Kosaka, H. Kobayashi, M. Ohashi, H. Yamauchi, and Y. Yamaguchi, J. Magn. Magn. Mater. **161**, 255 (1996).

[14] N. Uchida, H. Onodera, M. Ohashi, Y. Yamaguchi, N. Sato, and S. Funahashi, J. Magn. Magn. Mater. **145**, L16 (1995).

[15] J. K. Yakinthos, P. A. Kotsanidis, W. Schäfer, and G. Will, J. Magn. Magn. Mater. **89**, 299 (1990).

[16] J. K. Yakinthos, P. A. Kotsanidis, W. Schäfer, and G. Will, J. Magn. Magn. Mater. **102**, 71 (1991).

[17] J. K. Yakinthos, P. A. Kotsanidis, W. Schäfer, W. Kockelmann, G. Will, and W. Reimers, J. Magn. Magn. Mater. **136**, 327 (1994).

[18] N. P. Ong and J. W. Brill, Phys. Rev. B **18**, 5265 (1978).

[19] S. Shimomura *et al.* (unpublished).

[20] It was also confirmed by taking oscillation photographs that all the satellite peaks disappeared below T_C.

[21] P. Brüesch, *Phonons: Theory and Experiments II* (Springer-Verlag, Berlin, 1986).

[22] F. Galli, T. Taniguchi, A. A. Menovsky, G. J. Nieuwenhuys, J. A. Mydosh, and S. Ramakrishnan, Physica B (Amsterdam) **281–282**, 171 (2000).